Superconducting state in the ternary stannide superconductors $R_3T_4Sn_{13}$ (R = La, Sr; T = Rh, Ir) with a quasiskutterudite structure

N. Kase,* H. Hayamizu, and J. Akimitsu

Department of Physics and Mathematics, Aoyama-Gakuin University, Fuchinobe 5-10-1, Sagamihara, Kanagawa 229-8558, Japan

(Received 22 March 2010; revised manuscript received 20 January 2011; published 17 May 2011)

Single crystals of $R_3T_4Sn_{13}$ (R = La, Sr; T = Rh, Ir) are synthesized by a Sn-flux method. Superconducting transition temperatures T_c are determined on the basis of magnetic susceptibility and electrical resistivity measurements. For $La_3T_4Sn_{13}$, T_c = 3.1 and 2.5 K when T = Rh and Ir, respectively; similarly, for $Sr_3T_4Sn_{13}$, T_c = 4.2 and 5.0 K. Specific heat measurements indicate that superconducting gaps of these compounds are isotropic and that these superconductors can be categorized as strong-coupling superconductors on the basis of the values of $\Delta C_e/\gamma T_c$ and $2\Delta(0)/k_BT_c$. The upper critical field shows a clear enhancement with respect to the Werthamer-Helfand-Hohenberg prediction; this enhancement is consistent with the presence of a strong electron-phonon coupling. We summarized the normal and superconducting parameters of $R_3T_4Sn_{13}$ (R = La, Sr; T = Rh, Ir) in Table I.

DOI: 10.1103/PhysRevB.83.184509 PACS number(s): 74.25.Op, 74.25.F–

I. INTRODUCTION

The discovery of superconductivity in the ternary stannide compounds $R_3T_4Sn_{13}$ (cubic, so-called phase I) and $R_5T_6Sn_{18}$ (distorted cubic, so-called phase II) has attracted considerable attention as it facilitates a better understanding of the relationship between superconductivity and magnetism.[1] Magnetic transition is observed in the case of $R_5Rh_6Sn_{18}$ (R = Tb, Dy, Ho), and reentrant superconductivity is observed in the case of $R_5Rh_6Sn_{18}$ (R = Er, Tm); it is also observed that magnetic ordering destroys superconductivity in the region of superconducting transition temperature T_c > magnetic transition temperature T_M.[2–4]

The ternary stannides $Ca_3Rh_4Sn_{13}$ and $Yb_3Rh_4Sn_{13}$, which have a phase-I structure,[5] exhibit superconductivity at T_c ~8.0 K. The M-H curves of these compounds exhibit a peak effect[6,7] around $H_{c2}(T)$. While the phase-I structure of $Yb_3Rh_4Sn_{13}$ exhibits slight structural modifications owing to a disorder between the Sn and Yb sites, $Ca_3Rh_4Sn_{13}$ does not experience any such disorder, always adopting the phase-I structure.[8] This phase-I structure is closely related to the cage-type structure observed in filled skutterudites.[9]

$Sr_3T_4Sn_{13}$ (T = Rh and Ir) shows superconductivity at $T_c \sim 5 =$ K.[1] Although a previous study had reported on the occurrence of superconductivity in $Sr_3T_4Sn_{13}$, there has been no study that provides detailed information on the superconducting parameters of these materials. $La_3T_4Sn_{13}$ (T = Rh and Ir) shows superconductivity at $T_c \sim 3$ K.[1] The Rh-based superconductor $La_3Rh_4Sn_{13}$ is known to possess several critical temperatures in the range of 2.07–3.2 K.[1,10,11] The compound having T_c = 2.07 K is a strong-coupling superconductor as obtained from the expression $\Delta C_p/\gamma T_c \approx 2$.[10] Although several experiments have been performed on poly = single-crystalline samples in the Rh compound,[10,11] there has been no detailed investigation of the superconducting state of the Ir compound.

We successfully synthesized the single crystals of $R_3T_4Sn_{13}$ (R = Sr, La; T = Rh, Ir) in order to analyze its superconducting state. In this study, superconducting states of $R_3T_4Sn_{13}$ (R = Sr, La; T = Rh, Ir) were analyzed by measuring its magnetic susceptibility $\chi(T)$, magnetization $M(H)$, electrical resistivity $\rho(T)$, and specific heat $C(T)$ using the single crystals.

II. EXPERIMENTAL

Single crystals of $R_3T_4Sn_{13}$ (R = Sr, La; T = Rh, Ir) were synthesized by a Sn-flux method. The starting materials were La powder (99.9%), Sr bulk (99.9%), Rh powder (99.9%), Ir powder (99.9%), and Sn shot (99.999%). All the starting materials, having an off-stoichiometric composition of La or Sr : Rh or Ir : Sn = 1 : 1.33 : 10 were placed in an alumina crucible encapsulated in a quartz tube. The quartz tube was heated up to 1050, maintained at this temperature for approximately 3 h, and then cooled down to 200 at the rate of 5/h; this entire process takes 7 days. The Sn flux was removed by spinning the materials in a centrifuge; the centrifugation process removed most of the flux contamination from the surfaces of the single crystals; the remaining topical flux, if any, was etched using concentrated HCl. Many single crystals of $R_3T_4Sn_{13}$ have typical dimensions of 2.5 × 2.5 × 2.5 mm^3.

The single-crystalline nature of $R_3T_4Sn_{13}$ (R = Sr, La; T = Rh, Ir) was verified using a backscattring x-ray technique. The presence of well-defined Laue diffraction spots on the surface indicated the superior quality of the single crystals. As shown in Fig. 1, the crystal structure of the obtained polycrystalline sample was examined by the powder x-ray diffraction technique using a conventional x-ray spectrometer equipped with a graphite monochromator (RINT-1100 RIGAKU). Single crystal samples were crushed into a very fine powder and analyzed by powder x-ray diffraction by using Cu Kα radiation. The intensity data were collected by applying Cu Kα radiation to the sample over a 2θ range of 5°–80° with a step width of 0.02° and a counting time of 4°/minute. The JADE software is used to index all the peaks and to determine the lattice constants. The obtained powder x-ray diffraction patterns were indexed as the $R_3T_4Sn_{13}$ (R = La, Sr; T = Rh, Ir) phase with the space group $Pm\bar{3}n$. The lattice parameters were reported to be a = 0.97457(1) and 0.97550(3) nm where T = Rh and Ir, respectively; similarly, for $Sr_3T_4Sn_{13}$, these constants were determined to be a = 0.98048(3) and 0.98159(5) nm. These values are in good agreement with

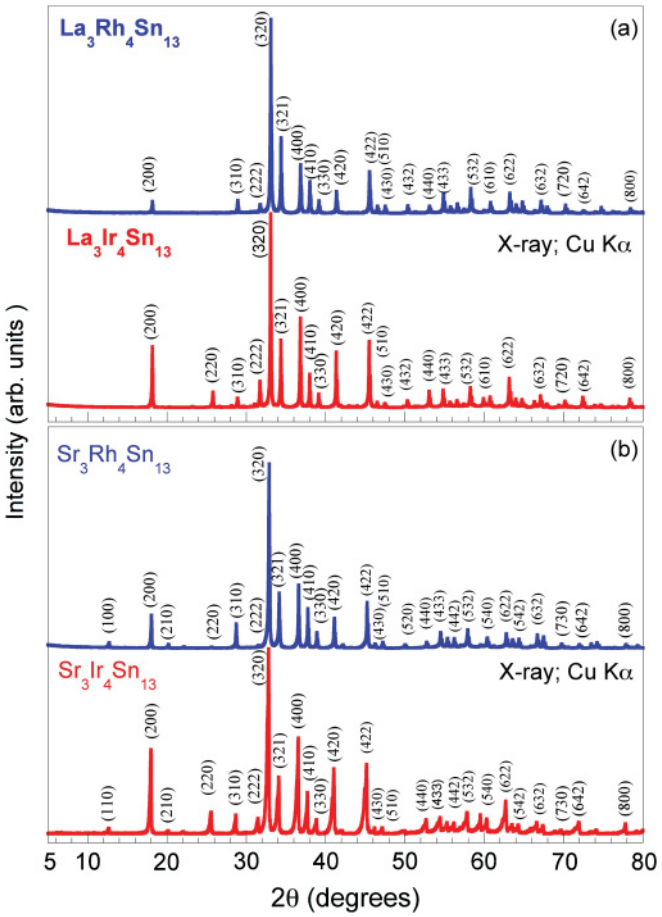

FIG. 1. (Color online) Powder x-ray diffraction pattern of (a) $La_3T_4Sn_{13}$ (T = Rh, Ir) and (b) $Sr_3T_4Sn_{13}$ (T = Rh, Ir).

previously reported data; the lattice parameters were reported to be $a = 0.9745$, 0.9751 nm for $La_3T_4Sn_{13}$ (T = Rh, Ir)[1] and $a = 0.9801$, 0.9807 nm for $Sr_3T_4Sn_{13}$ (T = Rh, Ir),[1] respectively.

The crystal compositions were determined by averaging the compositions of ten different regions of each crystal using an electron-probe microanalyzer equipped with wavelength dispersive spectrometers (EPMA-WDS; JEOL JXA8200S). The chemical composition of the samples was determined to be $La_{3.1(2)}Rh_{4.0(1)}Sn_{13.2(2)}$, $La_{3.1(1)}Ir_{4.0(1)}Sn_{13.6(2)}$, $Sr_{3.0(2)}Rh_{4.0(1)}Sn_{13.3(2)}$, and $Sr_{3.1(2)}Ir_{4.0(2)}Sn_{13.6(2)}$, respectively. These values are similar to the stoichiometric compositions of $R_3T_4Sn_{13}$, although the ratio of Sn is slightly large.

Magnetic susceptibility and other magnetization parameters were measured using a Superconducting Quantum Interference Device (SQUID) magnetometer (Quantum Design, MPMS) in a temperature range of 1.8–6.0 K under various applied magnetic fields. Electrical resistivity was measured by a conventional DC four-probe method in a temperature range of 0.4–7.0 K under zero magnetic field and various applied magnetic fields. Specific heat measurements were conducted using a Quantum Design Physical Property Measurement System (PPMS) equipped with a ^{3}He refrigerator in a temperature range of 0.4–6.0 K.

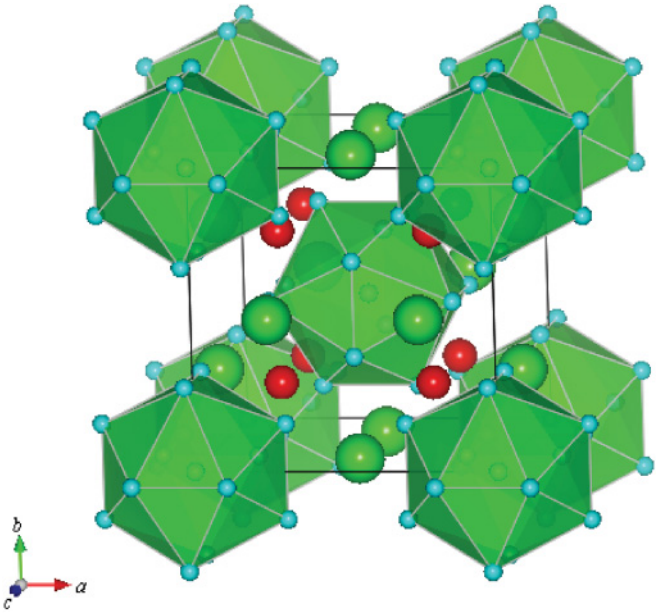

FIG. 2. (Color online) Crystal structure of $R_3T_4Sn_{13}$ (R = La, Sr; T = Rh, Ir). Sn1 is surrounded by the 12 × Sn2 cluster. The structure highlights the arrangement of the $Sn1(Sn2)_{12}$ icosahedra (light blue), with T atoms (red circles) bonding to Sn2 atoms to form trigonal prisms. For simplicity, the R atoms (green circles) are represented as isolated atoms. (The program VESTA is used.[32])

III. CRYSTAL STRUCTURE

$R_3T_4Sn_{13}$ (R = La, Sr; T = Rh, Ir) crystallizes to form a $Yb_3Rh_4Sn_{13}$-type structure[12] in the $Pm\bar{3}n$ space group (No. 223), as shown in Fig. 2. The lattice parameters were reported to be $a = 0.9745$ and 0.9751 nm for $La_3T_4Sn_{13}$ (T = Rh, Ir),[1] and $a = 0.9801$ and 0.9807 nm for $Sr_3T_4Sn_{13}$ (T = Rh, Ir),[1] respectively. The Sn_1 atoms occupy the origin of the unit cell and form edge-sharing $Sn_1(Sn_2)_{12}$ icosahedra which pack in a CsCl arrangement. The faces of each Sn_1 icosahedron in the network make contact with TSn_6 trigonal prisms and 12R-centered cuboctahedra-like. This feature is similar to the BO_6 octahedra in $AA_3B_4O_{12}$-type compounds[13,14] and also to the TPn_6 (Pn1/4 pnictogen) octahedra found in the structures of skutterudites such as $LaFe_4P_{12}$.[15]

IV. MAGNETIC PROPERTIES

$R_3T_4Sn_{13}$ (R = La, Sr; T = Rh, Ir) was found to exhibit superconductivity as it shows magnetic susceptibility $\chi(T)$ in a magnetic field of 10 Oe, as shown in Fig. 3. A large Meissner signal was clearly observed in the $\chi(T)$ curve below T_c = 4.2, 5.0 K for $Sr_3T_4Sn_{13}$ (T = Rh, Ir) and T_c = 3.1, 2.5 K for $La_3T_4Sn_{13}$ (T = Rh, Ir), respectively. While shielding by supercurrents comprises the whole sample volume (zero-field-cooled curves, considering demagnetizing factor and the high porosity of the samples) the field-cooling Meissner effect is less than unity. This incomplete Meissner effect is well known to be due to strong pinning.

The magnetic field dependence of magnetization $M(H)$ of $R_3T_4Sn_{13}$ (R = La, Sr; T = Rh, Ir) was observed at several temperatures; this dependence is shown in Fig. 4.

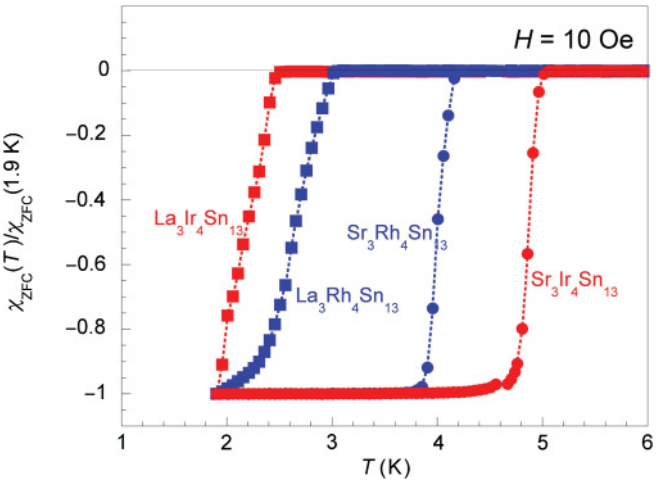

FIG. 3. (Color online) Temperature dependence of magnetic susceptibility $\chi(T)$ at 10 Oe in $R_3T_4Sn_{13}$ (R = La, Sr; T = Rh, Ir) normalized by the value at 2 K.

These compounds exhibited the butterfly curve, which is representative of the typical type-II superconducting behavior. We attempted to estimate the lower critical field $H_{c1}(0)$ at various temperatures using the M-H curve. However, because the temperature region is very narrow (above 1.8 K) for La compounds, we believe that the estimation of the lower critical field from the M-H curve will not provide accurate results. Hence, we estimated the lower critical field $H_{c1}(0)$ from the thermodynamic field using specific heat measurements.

V. SPECIFIC HEAT

The inset of Fig. 5 shows the temperature dependence of the specific heat C_p for La materials in the temperature range of 0.4–4.0 K under a zero and 3 T magnetic field and the same for Sr materials in the temperature range of 0.4–6.0 K under a zero and 5 T magnetic field. The bulk nature of the superconductivity and superior quality of the samples are confirmed by a sharp anomaly at T_c = 2.5 and 3.1 K for $La_3Ir_4Sn_{13}$ and $La_3Rh_4Sn_{13}$, respectively, and at T_c = 4.15 and 4.95 K for $Sr_3Rh_4Sn_{13}$ and $Sr_3Ir_4Sn_{13}$, respectively; these values are in good agreement with the values of T_c determined using $\chi(T)$.

A standard analysis is conducted under magnetic fields whose values exceed those of the upper critical fields; this analysis yields Sommerfeld constant γ and the Debye temperature Θ_D, which is calculated from $\beta = N(12/5)\pi^4 R\Theta_D^{-3}$, where R = 8.314 J/(K mol) and N = 20. To analyze the specific heat data, we use the expression $C_n(T) = \gamma T + \beta T^3 + \delta T^5$, where γT is the electronic contribution (= C_e), γ is the electronic specific heat coefficient (Sommerfeld constant), and $\beta T^3 + \delta T^5$ (= C_p) is contributed by phonons. However, the specific heat of Sr compounds under a magnetic field shows a fractional drop at a low-temperature region. Although the reason behind the anomaly is not clear (one of the reasons is the existence of rattling), the T^5 correlation term is certainly inadequate for a system containing an anomaly of phonons such as KOs_2O_6.[16] To fit the specific heat data, we use an equation with a correction term; this equation is given

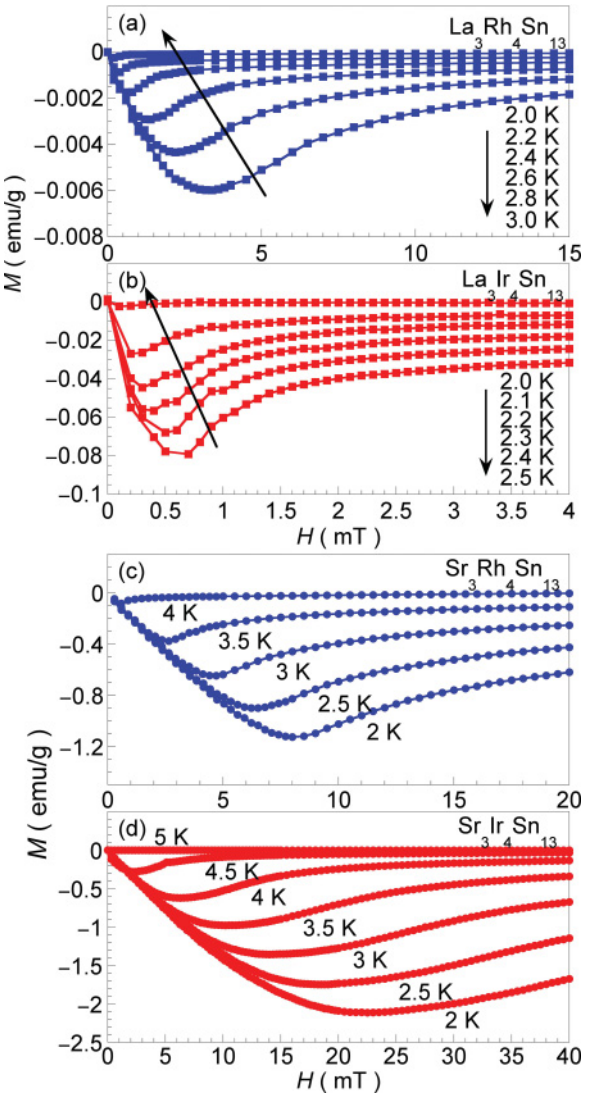

FIG. 4. (Color online) Magnetic field dependence of magnetization at several temperatures for (a) $La_3Rh_4Sn_{13}$, (b) $La_3Ir_4Sn_{13}$, (c) $Sr_3Rh_4Sn_{13}$, and (d) $Sr_3Ir_4Sn_{13}$.

as $C_n(T) = \gamma T + \beta T^3 + \sum_{n=2}^{4} \delta_{2n+1} T^{2n+1}$, where the third term is the correction term.[17] The obtained values of γ (mJ/K^2 mol) and Θ_D (K) are 22.2 and 284 for $La_3Rh_4Sn_{13}$, 19.2 and 296 for $La_3Ir_4Sn_{13}$, 31.0 and 252 for $Sr_3Rh_4Sn_{13}$, and 39.3 and 184 for $Sr_3Ir_4Sn_{13}$, respectively.

The solid curve of Fig. 5 represents the fitting result obtained by using the specific heat expression for a conventional superconductor ($C_e \sim \exp[-\Delta(0)/k_BT]$, where $\Delta(0)$ is the energy gap) below $0.8T_c$. Under a zero magnetic field, $C_e(T)$ behaves as an exponential dependence on temperature at low temperatures. From the exponential dependence curve, the superconducting energy gap $\Delta(0)$ (meV) at T = 0 can be estimated to be 0.505, 0.389 for $La_3T_4Sn_{13}$ (T = Rh, Ir) and 0.692, 0.870 for $Sr_3T_4Sn_{13}$ (T = Rh, Ir), respectively.

By using these values, we estimated $\Delta C_e/\gamma T_c$ to be approximately 1.84, 1.64 for $La_3T_4Sn_{13}$ (T = Rh, Ir), 1.78, 2.09 for $Sr_3T_4Sn_{13}$ (T = Rh, Ir), respectively. These values are relatively larger than those expected from the BCS theory ($\Delta C_e/\gamma T_c$ = 1.43). Moreover, $2\Delta(0)/k_BT_c$ is calculated to

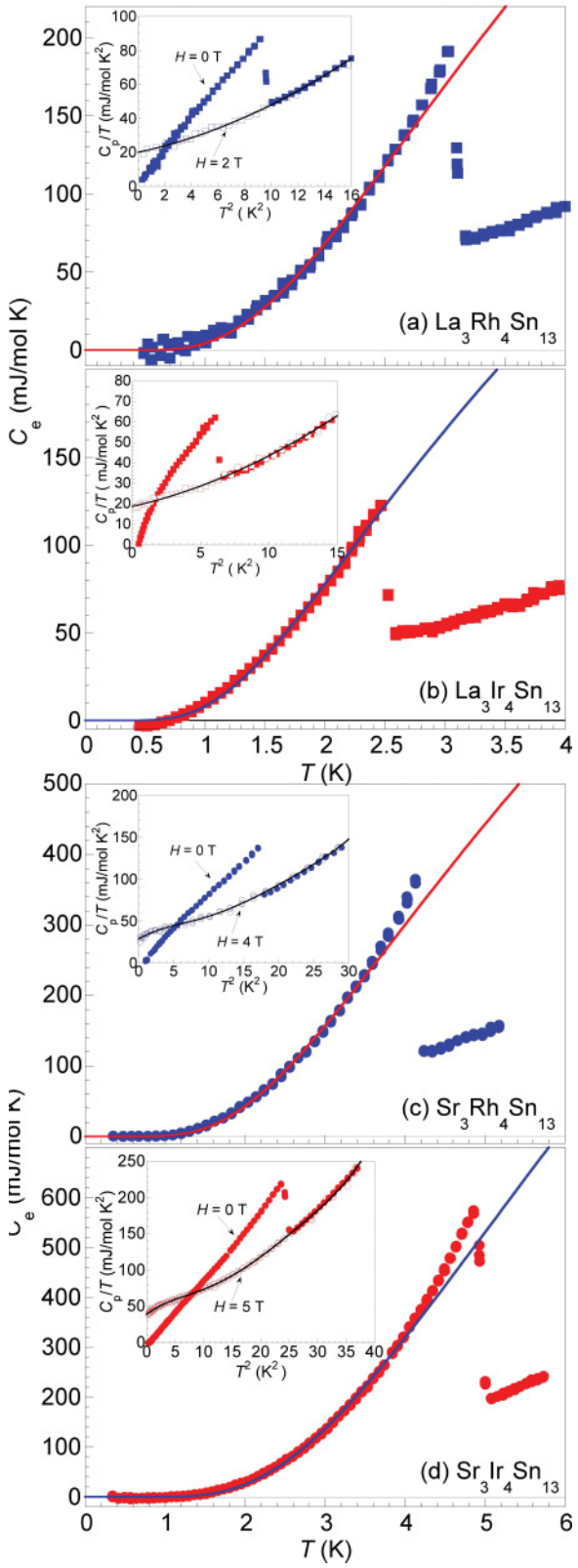

FIG. 5. (Color online) Temperature dependence of electronic specific heat C_e for (a), (b) $La_3T_4Sn_{13}$ (T = Rh, Ir) and (c), (d) $Sr_3T_4Sn_{13}$ (T = Rh, Ir). Solid lines represent an exponential dependence. Insets show temperature dependence of specific heat C_p/T. The solid line in the inset shows the fitting results of $C_n(T)$.

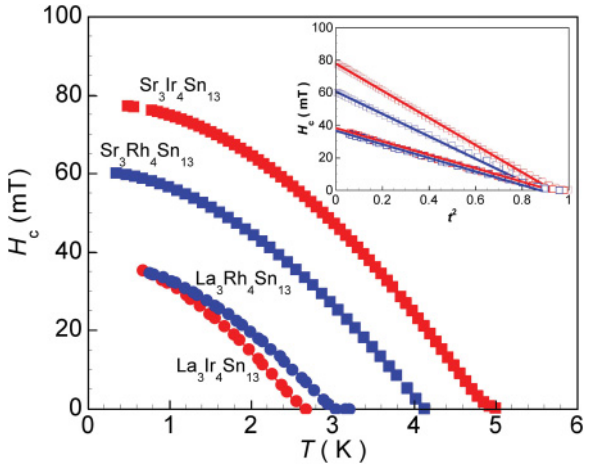

FIG. 6. (Color online) Thermodynamic critical field H_c. The inset shows H_c vs t^2; the solid line on each data set is a fit to the form $H_c = H_c(0)(1 - t^2)$ at a low-temperature limit.

be approximately 3.78, 3.61 for $La_3T_4Sn_{13}$ (T = Rh, Ir), and 3.87, 4.08 for $Sr_3T_4Sn_{13}$ (T = Rh, Ir), respectively. These values are also larger than those expected from the BCS theory $[2\Delta(0)/k_BT_c = 3.54]$. From these results, we concluded that all the materials can be categorized as strong-coupling superconductors.

The thermodynamic critical field $H_c(T)$ is one of the most important parameters for characterizing the nature of the superconducting ground state, because it is directly related to the condensation energy by the expression $\Delta F = \mu_0 H_c^2/8\pi$. $H_c(T)$ is deduced from the specific heat data obtained at $H = 0$ using the relation

$$\Delta F(T) = F_n - F_s = \frac{\mu_0 H_c^2(T)}{8\pi} = \int_{T_c}^{T} dT' \int_{T_c}^{T'} \frac{C_e}{T''} dT''. \quad (1)$$

The temperature dependence of $H_c(T)$ is shown in Fig. 6. As shown in the inset of Fig. 6, H_c follows the parabolic form $H_c = H_c(0)(1 - t^2)$ at low temperatures; $t = T/T_c$. $H_c(0)$ can be correctly determined unambiguously by an extrapolation to $T = 0$; the obtained values are $H_c(0) = 37.0$, 37.1 mT for $La_3T_4Sn_{13}$ (T = Rh, Ir) and $H_c(0) = 60.1$, 78.2 mT for $Sr_3T_4Sn_{13}$ (T = Rh, Ir), respectively.

VI. CRITICAL FIELDS

Figure 7 shows the temperature dependence of the resistivity under different magnetic fields up to $H = 3.5$ T. T_c is determined to decrease by 50% from the normal state resistivity value, and the transition width is taken as the temperature interval between 10% (T_c^{onset}) and 90% (T_c^{zero}) of the transition. In order to determine $H_{c2}(T)$ at low temperatures, the magnetoresistance was measured up to 3.5 T at different temperatures from 1.8 to 6 K (Fig. 7). The transition width gradually increases with increasing magnetic fields.

As shown in Fig. 8, the $H_{c2}(T)$ lines have a convex curve dependence for the overall temperature region; this behavior clearly deviates from that obtained by the Wertharmer-Helfand-Hohenberg (WHH) prediction.[18,19] Because of the invalidity for using these functions, we extrapolated the values

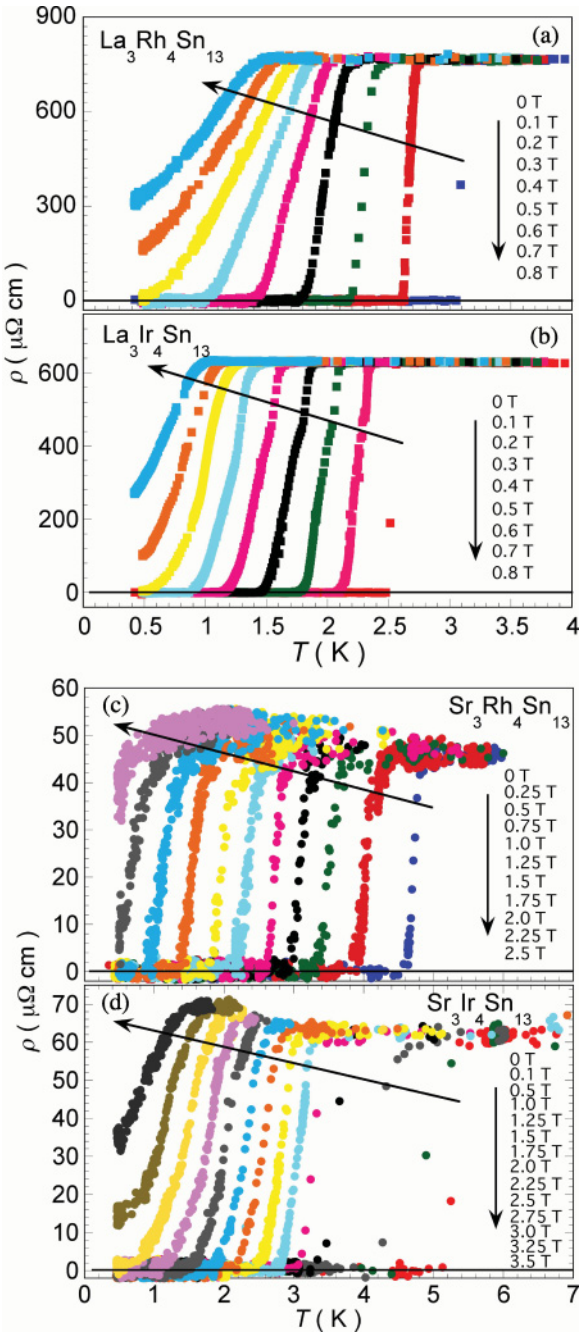

FIG. 7. (Color online) Temperature dependence of the electrical resistivity $\rho(T)$ under different applied magnetic fields for (a), (b) $La_3T_4Sn_{13}$ (T = Rh, Ir) and (c), (d) $Sr_3T_4Sn_{13}$ (T = Rh, Ir).

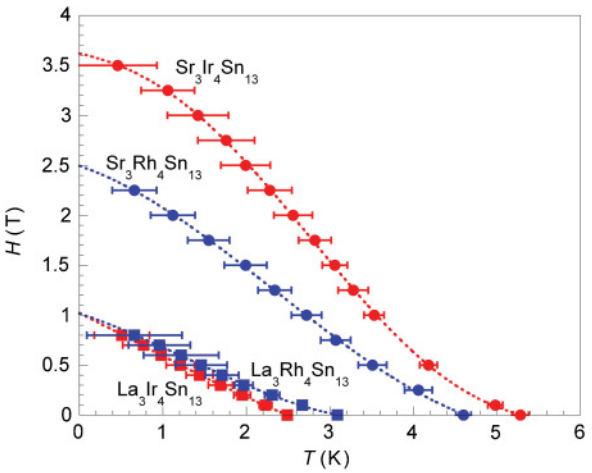

FIG. 8. (Color online) Temperature dependence of the upper critical fields $H_{c2}(0)$ for $Sr_3T_4Sn_{13}$ (T = Rh, Ir) determined from the electrical resistivity. The solid line represents the extrapolation to $T = 0$ by the polynomial function.

to $T = 0$ using the fifth power of the polynomial function of T. For $Sr_3T_4Sn_{13}$, the $H_{c2}(0)$ value was calculated to be approximately 2.50 and 3.54 T, where T = Rh and Ir, respectively. The $H_{c2}(0)$ value was calculated to be 1.02 for $La_3T_4Sn_{13}$, where T = Rh, Ir.

Such an enhancement of $H_{c2}(T)$ on the basis of the WHH prediction has been attributed to several different origins such as the localization effects in highly disordered superconductors,[20] anisotropy of the Fermi surface,[21] and strong electron-phonon coupling.[22,23] When the e-ph coupling is in the strong-coupling regime, $H_{c2}(T)$ starts to deviate from the WHH curve, remains linear as it moves toward lower temperatures, and finally has an upward curvature for a higher e-ph coupling. The present heat capacity measurements suggest that the $R_3T_4Sn_{13}$ (R = La, Sr; T = Rh, Ir) belongs to a strong-coupling BCS superconductor with an isotropic s-wave pairing symmetry. It is inferred from these results that H_{c2} enhancement cannot be because of the Fermi surface properties, but because of strong coupling. In addition, because these measurements were performed using pure single crystals, the localization effect due to impurity does not enhance the upper critical field.

On the basis of the $H_{c2}(0)$ and $H_c(0)$ values, we estimated the superconducting parameters for $R_3T_4Sn_{13}$ (R = La, Sr; T = Rh, Ir). According to the Ginzburg-Landau (GL) theory, the GL coherence length $\xi(0)$ and the GL parameter $\kappa(0) = \lambda(0)/\xi(0)$ can be obtained from the upper critical field $H_{c2}(0)$, the lower critical field $H_{c1}(0)$, and the thermodynamic critical field $H_c(0)$ using the following equations:

$$H_{c2}(0) = \frac{\Phi_0}{2\pi\xi(0)}, \tag{2}$$

$$H_{c1}(0) = \frac{H_c^2}{H_{c2}(0)}[\ln\kappa(0) + 0.08], \tag{3}$$

$$H_c(0) = \frac{H_{c2}(0)}{\sqrt{2}\kappa(0)}, \tag{4}$$

where Φ_0 is the flux quantum. With $H_{c2}(0)$ and $H_c(0)$, we obtained $\xi(0)$ and $\lambda(0)$ to be approximately 20.0 nm and 373 nm for $La_3Rh_4Sn_{13}$, 19.8 nm and 496 nm for $La_3Ir_4Sn_{13}$, 11.5 nm and 363 nm for $Sr_3Rh_4Sn_{13}$, and 9.65 and 328 nm for $Sr_3Ir_4Sn_{13}$, respectively. In addition, the GL parameter $\kappa(0)$ is calculated to be 15.7, 22.3 for $La_3T_4Sn_{13}$ (T = Rh, Ir) and 29.4, 32.0 for $Sr_3T_4Sn_{13}$ (T = Rh, Ir), respectively. These values indicate that these compounds are typical type-II superconductors. The measured and derived superconducting parameters are listed in Table I.

TABLE I. Superconducting and normal state parameters for $R_3T_4Sn_{13}$ (R = La, Sr; T = Rh, Ir).

	$La_3Rh_4Sn_{13}$	$La_3Ir_4Sn_{13}$	$Sr_3Rh_4Sn_{13}$	$Sr_3Ir_4Sn_{13}$
a (nm)	0.97457(1)	0.97550(3)	0.98048(3)	0.98159(5)
T_c (K)	3.1	2.5	4.2	5.0
$\mu_0 H_c(0)$ (mT)	37.0	27.9	60.1	78.2
$\mu_0 H_{c1}(0)$ (mT)	2.5	4.1	4.7	9.7
$\mu_0 H_{c2}(0)$ (T)	1.02	1.02	2.50	3.54
$\lambda(0)$ (nm)	401	509	363	328
$\xi(0)$ (nm)	18.0	18.0	11.5	9.65
$\kappa(0)$	19.5	25.9	29.4	32.0
γ (mJ/K^2 mol)	22.2	19.2	31.0	39.3
Θ_D (K)	284	296	252	184
$\Delta(0)$ (meV)	0.505	0.389	0.692	0.870
$\Delta C_e/\gamma T_c$	1.84	1.67	1.78	2.09
$2\Delta(0)/k_B T_c$	3.78	3.61	3.87	4.08

VII. DISCUSSION

In the case of e-ph coupled superconductors, Carbotte[24] has proposed that the characteristic thermodynamic quantities are computed using empirical formulas that can be described by one adjustable parameter, $x = \omega_{\ln}/T_c$; $\omega_{\ln}$ is the logarithmic averaged phonon frequency. These formulas are

$$\frac{\Delta C_e(T_c)}{\gamma T_c} = 1.43\left[1 + 53x^{-2}\ln\frac{x}{3}\right], \quad (5)$$

$$\frac{2\Delta(0)}{k_B T_c} = 3.54\left[1 + 12.5x^{-2}\ln\frac{x}{2}\right], \quad (6)$$

$$\frac{\gamma T_c^2}{H_c^2(0)} = 0.168\left[1 - 12.2x^{-2}\ln\frac{x}{3}\right]. \quad (7)$$

This analysis has been successfully applied to various metal-alloy superconductors;[24] to other recently discovered carbon-containing superconductors such as borocarbides,[25,26] $MgCNi_3$,[27] and La_2C_3;[28] and to rattling-induced superconductors.[16,29]

The thermodynamic quantities were estimated by varying $x = \omega_{\ln}/T_c$ in Eqs. (5), (6), and (7); they were estimated to be approximately 18.3, 20.2, and 24.7 for $La_3Rh_4Sn_{13}$; 26.3, 40.8, and 19.0 for $La_3Ir_4Sn_{13}$; 19.6, 16.5, and 11.8 for $Sr_3Rh_4Sn_{13}$; and 12.9, 11.9, and 19.0 for $Sr_3Ir_4Sn_{13}$, respectively. From the three values of x and T_c, we obtain mean value of $\hbar\omega_{\ln} = 65.3 \pm 5.9$, 71.8 ± 28 K for $La_3T_4Sn_{13}$ (T = Rh, Ir) and $\hbar\omega_{\ln} = 66.3 \pm 9.4$, 73.0 ± 11 K for $Sr_3T_4Sn_{13}$ (T = Rh, Ir), respectively. This $\omega_{\ln}$ value is only 20%~40% of the Debye temperature ω_D (200~300 K). The Debye frequency is determined only from the phonon DOS profile $F(\omega)$, while $\omega_{\ln}$ results are obtained on the basis of a weighting using the e-ph coupling function $\alpha^2(\omega)$. Such a reduced values of $\omega_{\ln}$ as compared to that of ω_D indicates the importance of the low-energy phonon modes for the superconductivity.

The electron-phonon coupling constant ($\lambda_{\rm ph}$) can be estimated using the well-known McMillan formula refined by Allen and Dynes:[24,30,31]

$$\lambda_{\rm ph} = \frac{1.04 + \mu^* \ln(\omega_{\ln}/1.2T_c)}{(1 - 0.62\mu^*)\ln(\omega_{\ln}/1.2T_c) - 1.04}, \quad (8)$$

where μ^* is the Coulomb pseudopotential and is fixed to be 0.10. The obtained values are estimated to be 0.805, 0.647 for $La_3T_4Sn_{13}$ (T = Rh, Ir) and 0.936, 0.983 for $Sr_3T_4Sn_{13}$ (T = Rh, Ir), respectively. Because of the calculated $\lambda \sim 1$, $Sr_3T_4Sn_{13}$ (T = Rh, Ir) can be categorized as a strong-coupling superconductor; this categorization is in good agreement with the results of specific heat measurements. In the case of $La_3T_4Sn_{13}$, the calculated values of λ are slightly lesser than 1.0, which is indicative of a moderate-coupling

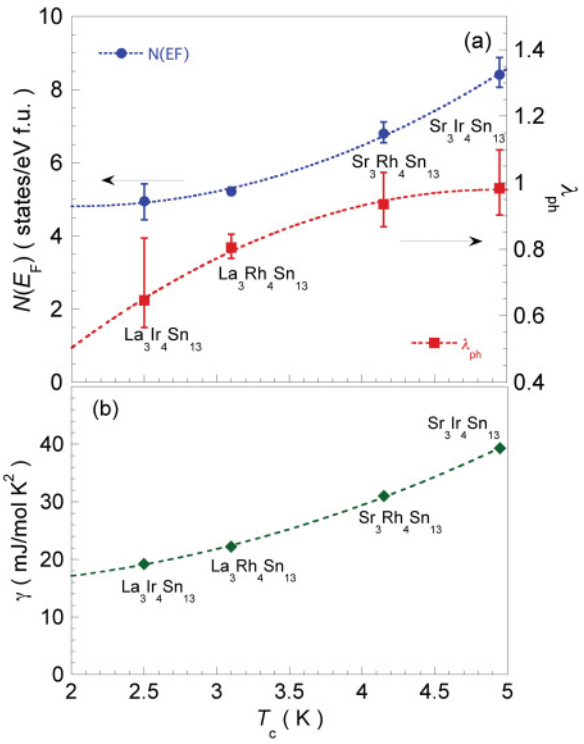

FIG. 9. (Color online) (a) $\lambda_{\rm ph}$, calculated using the modified McMillan formula and the density of states at the Fermi surface, as a function of temperature for $R_3T_4Sn_{13}$ (R = La, Sr; T = Rh, Ir). (b) Electronic specific heat coefficient (Sommerfeld constant) γ as a function of temperature.

superconductor. These results are almost consistent with those of specific heat measurements.

The electronic density of states at the Fermi level, $N(E_F)$, is expressed by the following relationship:

$$N(E_F) = \frac{3\gamma}{\pi^2 k_B^2 (1 + \lambda_{ph})}. \quad (9)$$

As shown in the above equation, $N(E_F)$ can be derived from the given γ and λ_{ph}. Using this relationship, we estimated $N(E_F)$ [states/(eV f.u.); f.u. denotes formula units] to be approximately 5.22, 4.95 for $La_3T_4Sn_{13}$ (T = Rh, Ir) and 6.80, 8.41 for $Sr_3T_4Sn_{13}$ (T = Rh, Ir), respectively. As shown in Fig. 9(a), both $N(E_F)$ and λ_{ph} increase with the transition temperature. The γ is increasing with increasing transition temperature, as shown in Fig. 9(b). Therefore, we assume that the difference in both $N(E_F)$ and λ_{ph} [$\gamma_{observed} = (1+\lambda)\gamma_{theoretical}$] results in a difference in superconducting transition temperatures.

In the previous report, the $N(E_F)$ of $La_3Rh_4Sn_{13}$ was obtained from band calculation with the LAPW method.[10] The calculated $N(E_F)$ is 5.58 states/(eV f.u.), which is in good agreement with that obtained from the above method. Thus, both the obtained $N(E_F)$ and λ_{ph} of $La_3Rh_4Sn_{13}$ are relatively reliable values.

In conclusion, we succeeded in synthesizing single crystals of $R_3T_4Sn_{13}$ (R = La, Sr; T = Rh, Ir) and analyzed the physical properties of these compounds by measuring their magnetic susceptibility $\chi(T)$, electrical resistivity $\rho(T)$, and magnetization $M(H)$. Specific heat measurements indicated that $R_3T_4Sn_{13}$ could be described as a conventional BCS superconductor in the strong-coupling regime. On the basis of the temperature dependence of C_e below T_c, we conclude that the symmetry of superconductivity of $R_3T_4Sn_{13}$ corresponds to an isotropic s-wave symmetry.

ACKNOWLEDGMENTS

This work was partially supported by "High-Tech Research Center Project" for Private Universities and a Grant-in-Aid for Scientific Research from the Ministry of Education, Culture, Sports, Science, and Technology, Japan. One of the authors (N.K.) acknowledges the support of the Iwanami Fujukai Foundation.

*n-kase@phys.aoyama.ac.jp

[1] J. P. Remeika, G. P. Espinosa, A. S. Cooper, H. Barz, Z. Fisk, L. D. Woolf, H. C. Hamaker, M. B. Maple, G. Shirane, and W. Thomlinson, Solid State Commun. **34**, 923 (1980).
[2] A. Rojek, C. Sulkowski, and K. Rogacki, Physica C **223**, 111 (1994).
[3] P. Bordet, S. Miraglia, J. L. Hodeau, and M. Marezio, J. Solid State Chem. **147**, 399 (1999).
[4] N. Kase, J. Akimitsu, Y. Ishii, T. Suzuki, I. Watanabe, M. Miyazaki, M. Hiraishi, S. Takeshita, and R. Kadono, J. Phys. Soc. Jpn. **78**, 073708 (2009).
[5] J. L. Hodeau, J. Chenavas, M. Marezio, and J. P. Remeika, Solid State Commun. **36**, 839 (1980).
[6] C. V. Tomy, G. Balakrishnan, and D. Mck. Paul, Physica C **280**, 1 (1997).
[7] C. V. Tomy, G. Balakrishnan, and D. M. Paul, Phys. Rev. B **56**, 8346 (1997).
[8] P. A. Westerveld, D. M. R. Lo Cascio, and H. Bakker, J. Phys. F **17**, 1963 (1987).
[9] W. Jeitschko and D. Braun, Acta Crystallogr. Sect. B **33**, 3401 (1977).
[10] M. Gamża, W. Schnelle, A. Ślebarski, U. Burkhardt, R. Gumeniuk, and H. Rosner, J. Phys. Condens. Matter **20**, 395208 (2008).
[11] U. Köhler, A. P. Pikul, N. Oeschler, T. Westerkamp, A. M. Strydom, and F. Steglich, J. Phys. Condens. Matter **19**, 386207 (2007).
[12] J. L. Hodeau, J. Chenavas, M. Marezio, and J. P. Remeika, Solid State Commun. **36**, 839 (1980).
[13] B. Bochu, M. N. Deschizeaux, J. C. Joubert, A. Collomb, J. Chenavas, and M. Marezio, J. Solid State Chem. **29**, 291 (1979).
[14] M. A. Subramanian, W. J. Marshall, T. G. Calvarese, and A. W. Sleight, J. Phys. Chem. Solids **64**, 1569 (2003).
[15] B. C. Sales, *Handbook on the Physics and Chemistry of Rare Earths* (Elsevier Science, Amsterdam, 2003), Vol. 33, p. 1.
[16] Z. Hiroi, S. Yonezawa, Y. Nagao, and J. Yamaura, Phys. Rev. B **76**, 014523 (2007).
[17] A. P. Petrovie, R. Lortz, G. Santi, C. Berthod, C. Dubois, M. Decroux, A. Demuer, A. B. Antunes, A. Pare, D. Salloum, P. Gougeon, M. Potel, and Ø. Fischer, e-print arXiv:1006.5956 (to be published).
[18] E. Helfand and N. R. Werthamer, Phys. Rev. **147**, 288 (1966).
[19] K. Maki, Phys. Rev. **148**, 362 (1966).
[20] L. Coffey, K. A. Muttalib, and K. Levin, Phys. Rev. Lett. **52**, 783 (1984); L. Coffey, K. Levin, and K. A. Muttalib, Phys. Rev. B **32**, 4382 (1985).
[21] T. Kita and M. Arai, Phys. Rev. B **70**, 224522 (2004).
[22] F. Marsiglio and J. P. Carbotte, Phys. Rev. B **41**, 8765 (1990).
[23] L. N. Bulaevskii, O. V. Dolgov, and M. O. Ptitsyn, Phys. Rev. B **38**, 11290 (1988).
[24] J. P. Carbotte, Rev. Mod. Phys. **62**, 1027 (1990).
[25] S. Manalo, H. Michor, M. El-Hagary, G. Hilscher, and E. Schachinger, Phys. Rev. B **63**, 104508 (2001).
[26] H. Michor, R. Krendelsberger, G. Hilscher, E. Bauer, C. Dusek, R. Hauser, L. Naber, D. Werner, P. Rogl, and H. W. Zandbergen, Phys. Rev. B **54**, 9408 (1996).
[27] A. Wälte, G. Fuchs, K.-H. Müller, A. Handstein, K. Nenkov, V. N. Narozhnyi, S.-L. Drechsler, S. Shulga, L. Schultz, and H. Rosner, Phys. Rev. B **70**, 174503 (2004).
[28] J. S. Kim, W.-H. Xie, R. K. Kremer, V. Babizhetskyy, O. Jepsen, and A. Simon, Phys. Rev. B **76**, 014516 (2007).
[29] Y. Nagao, J. Yamaura, H. Ogusu, Y. Okaoto, and Z. Hiroi, J. Phys. Soc. Jpn. **78**, 064702 (2009).
[30] W. L. McMillan, Phys. Rev. **167**, 331 (1968).
[31] P. B. Allen and R. C. Dynes, Phys. Rev. B **12**, 905 (1975).
[32] K. Momma and F. Izumi, Commission Crystallogr. Comput., IUCr Newslett. No. 7, 106 (2006).